Abyssal connections of Antarctic Bottom Water in a Southern Ocean State Estimate

Erik van Sebille,[1] Paul Spence,[1] Matthew R. Mazloff,[2] Matthew H. England,[1] Stephen R. Rintoul,[3,4,5] and Oleg A. Saenko[1,6]

Received 16 March 2013; revised 17 April 2013; accepted 17 April 2013; published 29 May 2013.

[1] Antarctic Bottom Water (AABW) is formed in a few locations around the Antarctic continent, each source with distinct temperature and salinity. After formation, the different AABW varieties cross the Southern Ocean and flow into the subtropical abyssal basins. It is shown here, using the analysis of Lagrangian trajectories within the Southern Ocean State Estimate (SOSE) model, that the pathways of the different sources of AABW have to a large extent amalgamated into one pathway by the time it reaches 31°S in the deep subtropical basins. The Antarctic Circumpolar Current appears to play an important role in the amalgamation, as 70% of the AABW completes at least one circumpolar loop before reaching the subtropical basins. This amalgamation of AABW pathways suggests that on decadal to centennial time scales, changes to properties and formation rates in any of the AABW source regions will be conveyed to all three subtropical abyssal basins. **Citation:** van Sebille, E., P. Spence, M. R. Mazloff, M. H. England, S. R. Rintoul, and O. A. Saenko (2013), Abyssal connections of Antarctic Bottom Water in a Southern Ocean State Estimate, *Geophys. Res. Lett.*, *40*, 2177–2182, doi:10.1002/grl.50483.

1. Introduction

[2] Antarctic Bottom Water (AABW) is the densest water mass found in the ocean, forming around Antarctica and filling the deepest parts of most of the Atlantic, Indian, and Pacific Oceans [*Orsi et al*., 1999, 2002; *Johnson*, 2008]. As the AABW reaches these abyssal ocean basins, this extremely cold and relatively freshwater mass is slowly entrained in the global thermohaline circulation [*Schmitz*, 1995; *Jacobs*, 2004].

[3] AABW forms in a number of localized and confined regions around Antarctica, the most important of which are the Weddell Sea [*Gill*, 1973], the Ross Sea [*Jacobs et al*., 1970], and the Mertz Polynya [*Rintoul*, 1998]. The temperature and salinity properties of these regional varieties—or water types—of bottom water are slightly different [e.g., *Worthington*, 1981; *Orsi et al*., 1999]. In the open ocean away from the source regions, however, the properties of AABW are observed to be much more uniform than close to the Antarctic shelf [*Orsi et al*., 1999], indicating that the different AABW varieties are eventually well mixed.

[4] The extent to which the types of AABW are homogenized in the Southern Ocean is particularly relevant when considering changes in AABW formation rates and properties between the different source regions [*Purkey and Johnson*, 2012]. Changes in Weddell Sea formation rates might, for example, be expected to have a greater impact on the stratification in the Atlantic Ocean than on that in the other oceans if most of the AABW formed in the Weddell Sea ends up in the Atlantic Ocean. If the different varieties of AABW were quickly homogenized, on the other hand, changes in one source region would be conveyed to all of the other ocean basins.

[5] One way to differentiate between these two scenarios is by studying a "connectivity matrix," which relates the source regions around Antarctica to the outflow regions in the subtropical basins. This requires a Lagrangian framework, where water parcels are tagged as they form AABW and then followed until they reach the subtropics. Ideally, the connectivity matrix would be formed using observations, but due to the time scales of abyssal flows (hundreds of years) and costs involved (thousands of floats), a numerical study is required. In this study, we use a state estimate of the Southern Ocean (the Southern Ocean State Estimate, SOSE) to study the abyssal connectivity of AABW and the associated pathways and time scales.

2. Methods

2.1. The Eulerian and Lagrangian Models

[6] The model used here, the Southern Ocean State Estimate (SOSE) [*Mazloff et al*., 2010], is a numerical model of the Southern Ocean based on ECCO Machinery [*Wunsch and Heimbach*, 2007] and constrained by a large set of in situ and remote-sensed observations in the Southern Ocean. Here the 5 day averaged three-dimensional velocity fields for the period January 2005 to December 2007 are used, on a 1/6° horizontal resolution and with 42 vertical levels. Constraints in the SOSE optimization limit abyssal stratification drift over the 3 year simulation, even though many of the observational data are limited to the upper 2000 m where ARGO data are available. The idealized Observation System

Additional supporting information may be found in the online version of this article.

[1]ARC Centre of Excellence for Climate System Science and Climate Change Research Centre, University of New South Wales, Sydney, NSW, Australia.
[2]Scripps Institute of Oceanography, La Jolla, California, USA.
[3]Centre for Australian Weather and Climate Research, Hobart, Tas, Australia.
[4]Antarctic Climate and Ecosystems Cooperative Research Centre, University of Tasmania, Hobart, Tas, Australia.
[5]Wealth From Oceans National Research Flagship, CSIRO, Hobart, Tas, Australia.
[6]Canadian Centre for Climate Modelling and Analysis, Environment Canada, Victoria, British Columbia, Canada.

Corresponding author: E. van Sebille, ARC Centre of Excellence for Climate System Science and Climate Change Research Centre, University of New South Wales, Sydney, NSW, Australia. (e.vansebille@unsw.edu.au)

0094-8276/13/10.1002/grl.50483

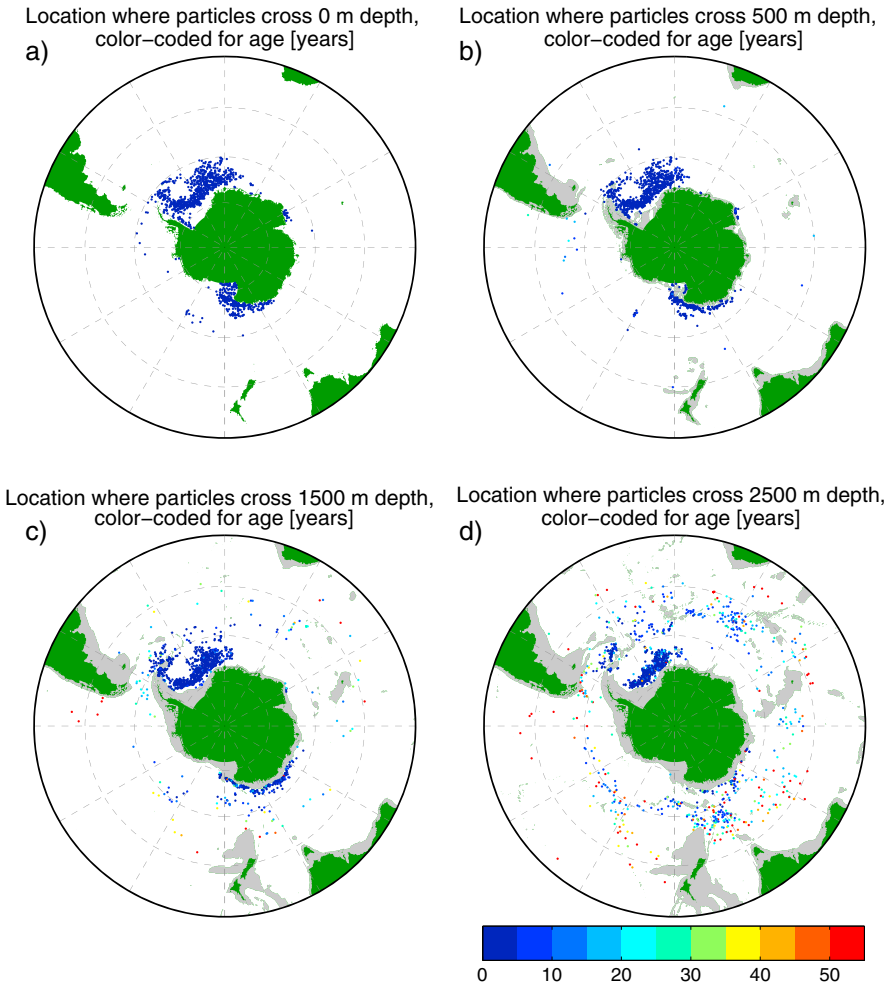

Figure 1. Locations and ages (in color) of the AABW particles at (a) formation and as they cross (b) the 500 m depth level, (c) the 1500 m depth level, and (d) the 2500 m depth level. Grey shaded in Figures 1b–1d are topographic features shallower than 500, 1500, and 2500 m, respectively. See also the movie in the supplementary material. When they reach 2500 m, most particles are within 10 years of formation and are still close to the Antarctic continental slope. However, 20% of the particles cross the 2500 m level within the ACC at ages above 25 years.

Simulation Experiment by *Forget et al.* [2008] revealed that constraining upper ocean fields limits deep ocean drift. While some stratification trends do still exist in SOSE, these are large scale with relatively weak horizontal gradients such that the effect on transport pathways is much smaller than any independent drift of temperature or salinity. SOSE has been extensively validated in the Southern Ocean [*Cerovečki et al.*, 2011; *Firing et al.*, 2011].

[7] To track the numerical particles through the three-dimensional velocity fields, we use the Connectivity Modeling System version 1.1 (CMS v1.1) [e.g., *van Sebille et al.*, 2012; *Paris et al.*, 2013]. The CMS integrates virtual particles within the SOSE velocity fields using a fourth-order Runge-Kutta scheme. In addition to this forward integration, CMS v1.1 has a novel mixed-layer parameterization to account for convective mixing. This is done because convective mixing within hydrostatic numerical ocean models involves implicit vertical mixing of the temperature and salinity fields outside any direct calculation of the velocity fields; models such as SOSE do not explicitly resolve the vertical velocities associated with convection [e.g., *Rahmstorf*, 1995]. This approach is similar to that previously applied by *Sen Gupta and England* [2004] in a diagnosis of bottom water pathways in eddy-permitting models.

[8] The mixed-layer parameterization of the CMS v1.1 mimics the convective signature in the velocity fields by adding a random Brownian motion component to the vertical position of the particles that are in the mixed layer. In essence, when a particle is diagnosed to be in the mixed layer (in SOSE defined to be the depth where the density is 0.05 kg/m^3 larger than the local surface density), the particle is randomly moved within the mixed layer (up to a maximum vertical velocity of 20 cm/s) before it is further advected with the local three-dimensional velocity fields. This parameterization allows for water mass formation both by advection across the base of the mixed layer and by mixed-layer shoaling.

[9] The particles are released every 5 days for a year, at 15 m depth, at each 0.5° of latitude and longitude poleward of 60°S. As we are interested in time scales beyond the 3 years of available data, we recycle the velocity fields by looping through them. *Van Sebille et al.* [2012] have successfully employed this technique to advect particles in NADW for two centuries. Here

we track the particles for a total of 500 years, a sufficiently long time for the particles to form AABW and to reach the subtropical basins (see also Figure 3b).

2.2. Selecting the AABW Particles

[10] Not all particles that are released form AABW. The large majority of the particles—particularly those released away from the Antarctic shelf—drift equatorward via the prevailing northward Ekman flow or do not sink to sufficiently high density classes. Here we remove the trajectories of those particles that do not reach deeper than the 28.27 kg/m^3 neutral density surface somewhere equatorward of 60°S. This 28.27 kg/m^3 isopycnal is generally considered the upper limit of unmixed Antarctic Bottom Water [e.g., *Orsi et al*., 1999].

[11] Of the particles that penetrate deeper than the 28.27 kg/m^3 isopycnal, only a very small number reach the subtropical basins at 31°S below that isopycnal. This is because the thickness of this layer rapidly decreases going equatorward, in agreement with the observational data presented in *Orsi et al*. [1999]. In the real ocean, most of the AABW gets diluted by overlying deep waters within the Southern Ocean [e.g., *Orsi et al*., 1999]. To account for this mixing of AABW on its way to the subtropical basins, we therefore retain those particles that, in neutral density coordinates, (1) penetrate below the 28.27 kg/m^3 isopycnal somewhere along their trajectory equatorward of 60°S and (2) end up below the 28.20 kg/m^3 isopycnal at 31°S. Note that choosing 28.00 kg/m^3 for this isopycnal at 31°S yields the same results and conclusions in this study, because condition (1) turns out to be the most stringent.

3. Results

3.1. Particle Pathways

[12] The pathways traced by only those particles that satisfy the conditions laid out above can best be appreciated by watching a movie of the first 50 years after they form. This movie is available in the supplementary material (8.5 MB). The initial frame of this movie (shown in Figure 1a) clearly shows three main areas of formation for the AABW particles, namely, in the Weddell Sea, in the Ross Sea, and along the coastline of eastern Antarctica. A few particles form as AABW somewhat farther offshore, but these account for less than 5% of the total amount of AABW particles.

[13] More than 60% of the AABW particles sink to depths below 500 m within a year and less than 100 km from their release locations (Figure 1b), predominantly along the Antarctic continental slope and near the regions where AABW is formed. From 500 m depth, most particles cascade further down to 1500 m depth (Figure 1c). In the Weddell Sea, the particles sink nearly vertically along the southern and western boundaries of the basin. Particles that sink in the Ross Sea move westward along the continental slope before turning eastward again at approximately 100°E (the movie in the supplementary material clearly shows this, too). This eastward retroflection in SOSE is in good agreement with the observation by *Orsi et al*. [1999] using CFC tracers, although these authors found the retroflection to be located slightly farther westward, at around 80°E.

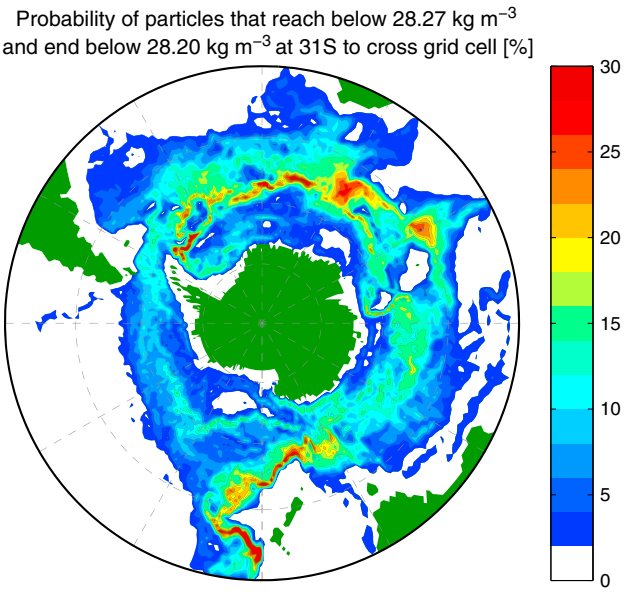

Figure 2. The pathway of AABW in the SOSE model. The map shows the percentage of particles that cross through each 1° × 1° grid cell at some time in the 500 year integration.

[14] Approximately a third of the particles travel a horizontal distance larger than 2000 km between 1500 and 2500 m depth levels (Figure 1d). These particles—particularly those formed outside the Weddell Sea—leave from the Antarctic continental slope and move into the Antarctic Circumpolar Current (ACC). Note that when these particles finally cross the 2500 m depth level, they are farther offshore and much older than the majority of the particles that have kept cascading down the continental slope.

[15] When all the particle trajectories are combined (Figure 2), the major pathways of AABW in the Southern Ocean are revealed. This figure shows, for each 1° × 1° box, the probability that a particle will visit that box at some time in the 500 year integration. A clear circumpolar pathway of the AABW particles, with relatively high probabilities marking the route of the ACC, can be observed at great depth (Figure 2). In general, the flow of AABW in SOSE appears to follow the pathways of relatively narrow and strong boundary currents, as also inferred from hydrography and current meter moorings [*Orsi et al*., 1999, 2002; *Fukamachi et al*., 2010].

[16] There are at least five distinct pathways out of the Southern Ocean and into the subtropical basins (Figure 2 and end of the movie in the supplementary material). In order of importance, they are east of New Zealand in the western Pacific Ocean (where 57% of the particles reach 31°S), around the Kerguelen Plateau in the central Indian Ocean (14%), in a broad region east of the 90°E Ridge in the eastern Indian Ocean (10%), in the Cape Basin in the eastern Atlantic Ocean (6%), and under the Agulhas Current in the western Indian Ocean (5%). The remaining 8% of the particles reach 31°S through much smaller pathways. Note, however, that these percentages only reflect where the particles reach 31°S and do not necessarily mean that they move further into the subtropical basins. The Cape Basin, for instance, is almost completely closed by the Walvis Ridge at depths of AABW, prohibiting further equatorward advection of AABW.

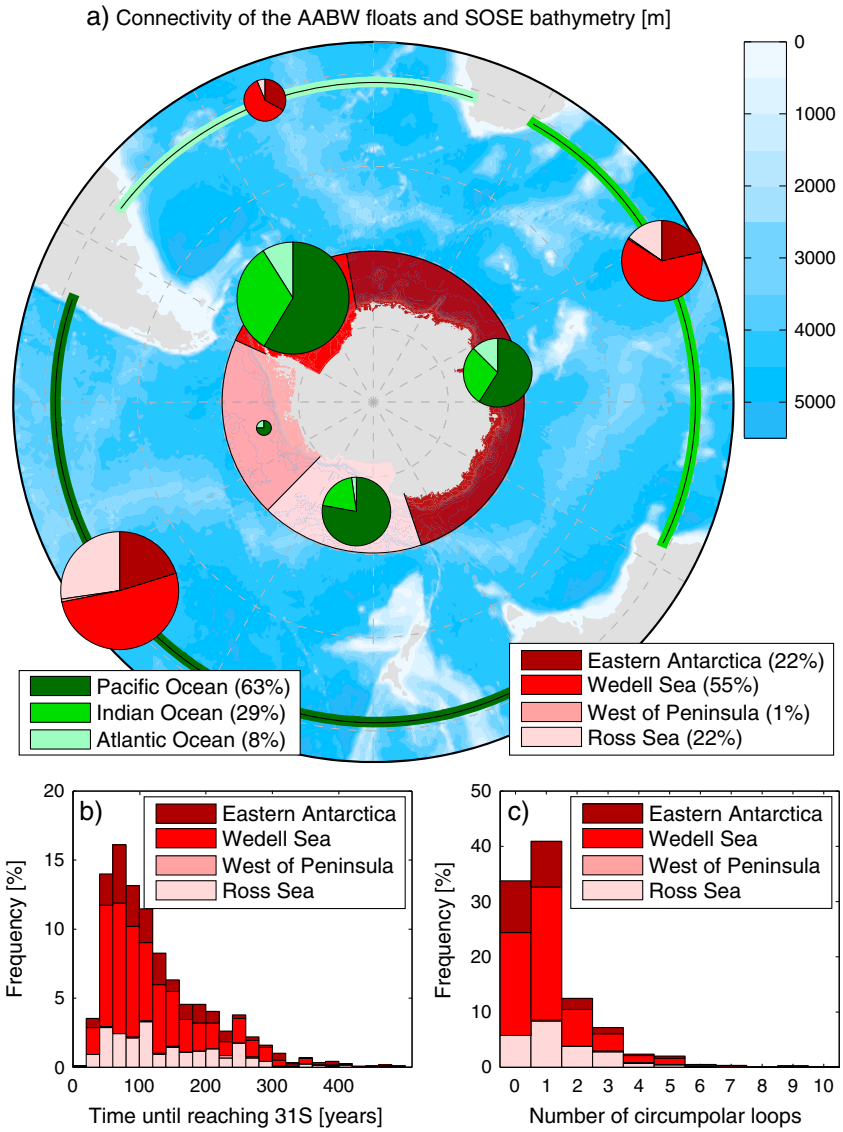

Figure 3. (a) The connectivity between the four formation regions and the three subtropical ocean basins as diagnosed from the Lagrangian particles on top of the bathymetry of the SOSE model in blue shading. The legends on the bottom show the percentage of particles that forms (right legend) and ends (left legend) on each of the sections, color coded on the map. The pie charts (the surface of which is scaled to the proportion of particles in that region) show for each of the four formation regions in which subtropical basins (green) the particles end and for each of the three end sections in which of the four formation regions (red) the particles form. This analysis suggests that the outflow distributions on the different formation and end sections are relatively similar, indicating a merging of bottom water types within the Southern Ocean. (b) The time it takes the particles to reach the abyssal ocean at 31°S from their formation region, color coded for the source regions. Most particles reach 31°S within 100 years. (c) The number of circumpolar loops made by the particles before they reach 31°S, also color coded for the source regions. Most particles perform at least one circumpolar loop.

[17] The ocean basin partition of Lagrangian inflow in the model is in remarkable agreement with the observational data of *Johnson* [2008], who found that of the volume of AABW north of the sub-Antarctic front, 70%, 23%, and 8% reside in the Pacific, Indian, and Atlantic Oceans, respectively (G. Johnson, personal communication). Although the inflow into the basins from the south need not be partitioned in the exact same way as the total volume in each basin, these ratios are very close to the Lagrangian transport partitioning in this study, namely, 63%, 29%, and 8%, for the Pacific, Indian, and Atlantic sections at 31°S, respectively.

3.2. Particle Connectivity and Pathway Amalgamation

[18] The connectivity between the four source regions around Antarctica and the three subtropical basins is high (Figure 3). The green pie charts close to Antarctica show that AABW from each of the four source regions shares a similar fate, namely, 60%–80% of the particles end up in the Pacific, 20%–30% of the particles end up in the Indian, and 5%–10% of the particles end up in the Atlantic Oceans, irrespective of where the particles are formed. Similarly, the contribution of each source to the AABW that crosses 31°S in each basin (the red pie charts) also shows merger of the source particles,

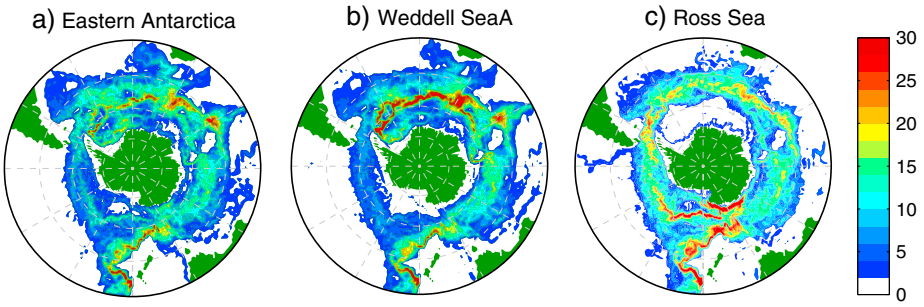

Figure 4. The pathway of AABW in the SOSE model, as a function of the three major source regions. The map is very similar to that of Figure 2 and shows the percentage of particles that cross through each 1° × 1° grid cell at some time in the 500 year integration for the particles formed in (a) eastern Antarctica, (b) the Weddell Sea, and (c) the Ross Sea. Equatorward of 60°S, the pathways are very similar for the three source regions (with pointwise correlations ranging from 0.74 between the Ross Sea and eastern Antarctica sources to 0.95 between the Weddell Sea and eastern Antarctica sources), indicating a high degree of amalgamation of AABW pathways in the Southern Ocean.

with AABW exported from the Weddell Sea making the dominant contribution in each basin.

[19] More evidence for the effective mixing of particles from the different source regions can be found in the amalgamation of the export pathways. AABW from each of the three main sources follows a similar pathway (Figure 4), especially equatorward of 60°S where most amalgamation occurs. Irrespective of where the particles form, their main export pathway is consistently east of New Zealand. Furthermore, most AABW particles formed in each of the source regions tend to do at least one circuit of Antarctica before spreading north to the subtropics (Figure 3c), resulting in a clear circumpolar pathway for all three source regions (Figure 4). The largest differences between the different panels in Figure 4 are that particles formed in the Ross Sea have a stronger tendency to cross the South Pacific (see also Figure 3c), likely because particles formed in the Ross Sea are quickly swept eastward and complete at least one circuit of Antarctica before entering the South Pacific east of New Zealand.

[20] The differences in the pathways from the different source regions—and thus the degree of pathway amalgamation—can be quantified. The pathways of the particles formed in the Ross Sea differ most from those formed in the other two source regions (Figure 4), but the pointwise correlation between grid cell values equatorward of 60°S of the particles formed in the Ross Sea with the particles formed in the Weddell Sea and around eastern Antarctica is still 0.74 and 0.84, respectively. The equivalent correlation between the pathways of the particles formed in the Weddell Sea and those formed in East Antarctica is even higher, at 0.95, confirming that AABW formed in the Weddell Sea has a very similar fate to that formed around eastern Antarctica.

4. Discussion

[21] This analysis of the connectivity between regions of AABW formation and the subtropical basins, using Lagrangian particles in the SOSE data-assimilating model, suggests that the pathways of the distinct sources of AABW amalgamate in the Southern Ocean, such that the three sources of AABW have to a large extent merged by the time it is exported across 31°S.

[22] Strong advection by the ACC can explain the relatively similar contributions of each source region to the subtropical basins. This role of the ACC in transporting and amalgamating the pathways of AABW is also evident in the finding that almost 70% of the particles take one or more loops around the deep ACC on their journey between the surface oceans around Antarctica and the abyssal subtropical basins (Figure 3c).

[23] Most of the locations where the AABW particles cross the Antarctic Circumpolar Current (Figure 2) seem to correspond with either deep western boundary currents or with locations of enhanced cross-jet mixing in the upper ocean [see, for example, *Thompson and Sallée*, 2012, Figure 10]. It might thus be that these jets have some influence on the deep circulation, which could be further evidence that mixing in the Southern Ocean plays an important role in the export of AABW. A dedicated study on this subject is currently underway.

[24] Somewhat surprisingly, 63% of the AABW particles end up in the Pacific Ocean (Figure 3), predominantly through the pathway east of New Zealand (Figures 2 and 4), whereas only 8% of the particles end up in the Atlantic Ocean. Although part of this difference in inflow between the Pacific and Atlantic might be explained by the basin surface area (which sets the potential for diapycnal upwelling) and zonal length of the connection to the Southern Ocean (which sets the potential for equatorward intrusions), the Pacific Ocean seems to be overrepresented in the end basins of AABW particles. Future modeling and observational studies might be able to shed light on this finding and help determine how well this feature is represented within SOSE.

[25] The main finding of this study, that bottom waters from different source regions are to a large extent amalgamated into one AABW within the Southern Ocean, is relevant when studying changes in the formation rates of the different varieties of bottom water. Changes in the properties of the Weddell Sea, for example, will be transmitted by advective signals on decadal to centennial time scales (Figure 3b) to all of the subtropical ocean basins, although it is important to note in this respect that water property changes around Antarctica are also communicated by radiation of Rossby and Kelvin waves [e.g., *Coles et al.*, 1996; *Masuda et al.*,

2010], which can significantly reduce the dynamical response time.

[26] The Lagrangian advective pathways described here imply that changes in any one of the source regions (such as observed by *Purkey and Johnson* [2012]) will be also diluted if the other source regions do not change. This ultimately has implications for climate change detection and attribution in the abyssal ocean.

[27] **Acknowledgments.** This project was supported by the Australian Research Council via grants DE130101336, FL100100214, and CE110001028. This work was also supported in part by the Australian Government's Cooperative Research Centres Program, through the Antarctic Climate and Ecosystems Cooperative Research Centre (ACE CRC), and by the Department of Climate Change and Energy Efficiency through the Australian Climate Change Science Program. Computational resources for the SOSE were provided by NSF XSEDE resource grant MCA06N007. We thank Gregory C. Johnson for providing data on the partitioning of AABW volumes in the three basins and suggestions on how to improve the manuscript.

[28] The Editor thanks Gregory Johnson and an anonymous reviewer for their assistance in evaluating this paper.

References

Cerovečki, I., L. D. Talley, and M. R. Mazloff (2011), A comparison of Southern Ocean air-sea buoyancy flux from an ocean state estimate with five other products, *J. Clim.*, *24*(24), 6283–6306, doi:10.1175/2011JCLI3858.1.

Coles, V. J., M. S. McCartney, D. Olson, and W. M. Jr.Smethie (1996), Changes in Antarctic Bottom Water properties in the western South Atlantic in the late 1980s, *J. Geophys. Res.*, *101*, 8957–8970.

Firing, Y. L., T. K. Chereskin, and M. R. Mazloff (2011), Vertical structure and transport of the Antarctic Circumpolar Current in Drake Passage from direct velocity observations, *J. Geophys. Res.*, *116*, C08015, doi:10.1029/2011JC006999.

Forget, G., B. Ferron, and H. Mercier (2008), Combining Argo profiles with a general circulation model in the North Atlantic. Part 1: Estimation of hydrographic and circulation anomalies from synthetic profiles, over a year, *Ocean Modell.*, *20*(1), 1–16, doi:10.1016/j.ocemod.2007.06.001.

Fukamachi, Y., S. R. Rintoul, J. A. Church, S. Aoki, S. Sokolov, M. A. Rosenberg, and M. Wakatsuchi (2010), Strong export of Antarctic Bottom Water east of the Kerguelen plateau, *Nat. Geosci.*, *3*(5), 327–331, doi:10.1038/NGEO842.

Gill, A. E. (1973), Circulation and bottom water production in the Weddell Sea, *Deep Sea Res.*, *20*(2), 111–140.

Jacobs, S. S. (2004), Bottom water production and its links with the thermohaline circulation, *Antarct. Sci.*, *16*(04), 427–437, doi:10.1017/S095410200400224X.

Jacobs, S. S., A. F. Amos, and P. M. Bruchhausen (1970), Ross sea oceanography and Antarctic Bottom Water formation, *Deep Sea Res.*, *17*(6), 935–962, doi:10.1016/0011-7471(70)90046-X.

Johnson, G. C. (2008), Quantifying Antarctic Bottom Water and North Atlantic Deep Water volumes, *J. Geophys. Res.*, *113*, C05027, doi:10.1029/2007JC004477.

Masuda, S., et al. (2010), Simulated rapid warming of abyssal North Pacific waters, *Science*, *329*, 319–322, doi:10.1126/science.1188703.

Mazloff, M. R., P. Heimbach, and C. Wunsch (2010), An eddy-permitting Southern Ocean State Estimate, *J. Phys. Oceanogr.*, *40*(5), 880–899, doi:10.1175/2009JPO4236.1.

Orsi, A. H., G. C. Johnson, and J. L. Bullister (1999), Circulation, mixing, and production of Antarctic Bottom Water, *Prog. Oceanogr.*, *43*(1), 55–109.

Orsi, A. H., W. M. Smethie Jr., and J. L. Bullister (2002), On the total input of Antarctic waters to the deep ocean: A preliminary estimate from chlorofluorocarbon measurements, *J. Geophys. Res.*, *107*(C8), 3122, doi:10.1029/2001JC000976.

Paris, C. B., J. Helgers, E. van Sebille, and A. Srinivasan (2013), Connectivity Modeling System: A probabilistic modeling tool for the multi-scale tracking of biotic and abiotic variability in the ocean, *Environ. Modell. Software*, *42*, 47–54, doi:10.1016/j.envsoft.2012.12.006.

Purkey, S. G., and G. C. Johnson (2012), Global contraction of Antarctic Bottom Water between the 1980s and 2000s, *J. Clim.*, *25*(17), 5830–5844, doi:10.1175/JCLI-D-11-00612.1.

Rahmstorf, S. (1995), Multiple convection patterns and thermohaline flow in an idealized OGCM, *J. Clim.*, *8*(12), 3028–3039.

Rintoul, S. R. (1998), *On the origin and influence of Adelie Land Bottom Water*, Antarctic Research Series.

Schmitz, W. J., Jr. (1995), On the interbasin-scale thermohaline circulation, *Rev. Geophys.*, *33*(2), 151–173.

Sen Gupta, A., and M. H. England (2004), Evaluation of interior circulation in a high-resolution global ocean model. Part I: Deep and bottom waters, *J. Phys. Oceanogr.*, *34*(12), 2592–2614.

Thompson, A. F., and J.-B. Sallée (2012), Jets and topography: Jet transitions and the impact on transport in the Antarctic Circumpolar Current, *J. Phys. Oceanogr.*, *42*, 956–972, doi:10.1175/JPO-D-11-0135.1.

Worthington, L. V. (1981), *The Water Masses of the World Ocean: Some Results of a Fine-Scale Census*, edited by B. Warren and C. Wunsch, pp. 42–69, MIT Press, Cambridge.

Wunsch, C., and P. Heimbach (2007), Practical global oceanic state estimation, *Phys. Nonlinear Phenom.*, *230*(1–2), 197–208, doi:10.1016/j.physd.2006.09.040.

van Sebille, E., W. E. Johns, and L. M. Beal (2012), Does the vorticity flux from Agulhas rings control the zonal pathway of NADW across the South Atlantic? *J. Geophys. Res.*, *117*, C05037, doi:10.1029/2011JC007684.